Journal of Contemporary Studies in Science and Innovation (JCSSI)
Journal Page: https://debracollege.ac.in/jcssi/index.aspx

Epigenetic Therapeutic Potential of Dulcitol, a Sugar Alcohol, as a Multi-Target HDAC Inhibitor against cervical cancer: Insights from In Silico Investigations

Kakali Sarkar[1], Maria Debbarma[1], Aishi Chakraborty[1], Sudhan Debnath[2], Samir Kumar Sil[1*]

[1]Department of Human Physiology, Tripura University, Suryamaninagar, Tripura (West), 799022, India
[2]Department of Chemistry, Netaji Subhash Mahavidyalaya, Udaipur, Gomati, Tripura, 799114, India

Abstract

Recent studies have highlighted dulcitol (galactitol), a natural sugar alcohol, as a promising molecule with emerging anticancer potential. It has been shown that it promotes apoptosis, modulates oxidative stress and autophagic pathways, and inhibits proliferation, migration, and metastasis in multiple cancer types, such as glioma, hepatocellular, and triple-negative breast cancers. Histone deacetylase (HDAC) inhibitors are emerging as key "epigenetic weapons" against cancer. However, until now none of the studies have explored the role of dulcitol in epigenetic regulation through inhibition of HDACs. This study, therefore, was designed to evaluate the epigenetic regulatory role of dulcitol as a multi-target inhibitor of HDAC2, HDAC3, and HDAC8—key epigenetic modulators overexpressed in cervical cancer—through in silico analysis. Molecular docking showed that this multi-targeted inhibitor had stronger binding affinities than that of the FDA-approved inhibitors, interacting with key amino acids and the Zn^{2+} ion in active sites. ADMET analysis confirmed its favorable safety profile, with no significant hepatotoxicity, carcinogenicity, mutagenicity, immunogenicity or cytotoxicity. Additionally, molecular dynamics simulations demonstrated very stable HDAC-dulcitol interactions over 100 ns. This study provides strong in silico evidence for considering this sugar alcohol as a novel epigenetic therapeutic candidate for cervical cancer, though further experimental validation is warranted.

Keywords: Dulcitol; Multi-targeted inhibitor; Histone deacetylase; Cervical cancer

***Corresponding author:**
Email address: s_k_sil@tripurauniv.ac.in
DOI: https://doi.org/10.5281/zenodo.18230300
Received on: 12 December 2025; Accepted on: 16 December 2025

1. Introduction

Histone deacetylase (HDAC) inhibitors have lately emerged as "epigenetic weapons" in the war of cancer. HDAC inhibitors reverse the abnormal protein acetylation in cancer cells and can restore the expression of tumor suppressors, leading to cell-cycle arrest, apoptosis, and suppression of angiogenesis, differentiation and metastasis (Li and Seto, 2016). Cancer cells are also reported to be more sensitive to apoptosis induced by HDAC inhibitors in comparison to normal cells (Ungerstedt et al., 2005), providing additional therapeutic potential of HDAC inhibitors and thereby, building a solid rationale for targeting HDACs in cancer therapy. Over-expression of HDACs has been found to be significantly linked to various human cancers, making these over expressed proteins a promising target for cancer treatment (Alseksek et al., 2022).

Recent studies have revealed the over expression of HDAC2 (Huang et al., 2005; Lin et al., 2009), HDAC3 (Zhang et al., 2016; Sun et al., 2022) and HDAC8 (Vanaja et al., 2018) in cervical cancer cell lines. Notably, downregulating HDAC2 protein expression was shown to inhibit HeLa cell proliferation and arrest the cell cycle, leading to cervical cancer cell death, underscoring the importance of its inhibition in cervical cancer (Hua et al., 2012). Additionally, HDAC2 knockdown led to an increase in apoptosis of cervical cancer cells (Huang et al., 2005) and pharmacological inhibiton of HDAC2 was found to slow cervical cancer cell growth (Lin et al., 2009). Elevated HDAC2 expression has also been observed in cervical dysplasia and cervical carcinoma, further highlighting its significance in the progression of cervical cancer (Huang et al., 2005; Lin et al., 2009). Similarly, significant down-regulation of the expression of mRNA and protein levels of HDAC3 was observed following transfection of the HDAC3 siRNA and a positive association was correlated between HDAC3 protein expression and cervical cancer differentiation, myometrial invasion, and lymph node metastasis (Zhang et al., 2016). Furthermore, HDAC8 knockdown via RNA interference inhibited cervical cancer cell growth and pharmacological inhibition of HDAC8 significantly decreased the migrational efficiency and reduced the mitotic phase of cervical cancer cells, highlighting its critical role in cancer cell proliferation, growth, and migration (Vannini et al., 2004). These findings highlight the potential of targeting these HDACs in cervical cancer treatment.

Despite advancements in anticancer research, resistance and toxicity issues highlight the urgent need for novel, effective, and safer therapeutic agents. In this context natural compounds are increasingly explored as promising sources of anticancer candidates due to their structural diversity and bioactivity. Among these, polyols, a class of sugar alcohols, have been reported to influence cancer cell behaviour by modulating oxidative stress, metabolic pathways and apoptosis, though their precise mechanisms and therapeutic potential remain underexplored.

Dulcitol is extensively used as a herbal medicine in Asia for thousands of years (Sha et al., 2018). It has multiple biological functions, including anti-inflammatory (Kobayashi et al., 1997), antioxidant (Erukainure et al., 2019), and anticancer properties (Zhang et al., 2020; Lin et al., 2020). However, until now none of the studies have explored the role of dulcitol in epigenetic regulation of cervical cancer progression through inhibition of HDACs. Therefore, the present *in silico* study was designed to evaluate the regulatory role of dulcitol targeting

HDACs that are overexpressed in cervical cancer.

2. Materials and Methods

2.1. Dataset preparation

The 3D X-ray crystal structures of multiple HDACs were fetched from the RCSB PDB (`https://www.rcsb.org/`) including HDAC1 (PDB ID: 4BKX; resolution: 3.0 Å) (Millard et al., 2013), HDAC2 (PDB ID: 3MAX; resolution: 2.05 Å) (Bressi et al., 2010), HDAC3 (PDB ID: 4A69; resolution: 2.06 Å) (Watson et al., 2012), HDAC4 (PDB ID: 2VQM; resolution: 1.8 Å) (Bottomley et al., 2008), HDAC6 (PDB ID: 5WPB; resolution: 1.55 Å) (Harding et al., 2017) and HDAC8 (PDB ID: 1T64; resolution: 1.90 Å) (Somoza et al., 2004). The 3D structures of five standard FDA-approved HDAC inhibitors were retrieved from the PubChem database (`https://pubchem.ncbi.nlm.nih.gov`) in `.sdf` format.

2.2. Protein preparation and receptor grid box generation

The X-ray crystal structures of multiple PDB IDs of HDACs namely 4BKX, 3MAX, 4A69, 2VQM, 5WPB and 1T64 were prepared using the Protein Preparation Wizard workflow in Maestro 13.4 (Schrödinger, LLC, New York, NY, 2022–4). During protein preparation, the protein structures were first cleaned by removing all water molecules to avoid any unnecessary interactions during docking simulations. Then missing hydrogens and loops were added to the protein and co-ligand. The energy of the protein–ligand complexes was minimized using the OPLS_2005 force field until the root-mean-square deviation (RMSD) between the minimized structure and the initial structure was reduced to 0.30 Å(Sastry et al., 2013). This step ensured that the proteins were in stable conformation before further analysis. For all HDACs except HDAC1, a receptor grid box of 15.0 Å cube was constructed by choosing the co-ligand of the active site. For HDAC1, the grid box was generated by selecting the active site amino acid residues ASP-264, ASP-176, and HIS-178 (Pidugu et al., 2016).

2.3. Ligand preparation

The 3D structures of dulcitol including the five standard HDAC inhibitors were imported in Maestro. The ligands were geometrically optimized using the LigPrep module of Schrödinger, with energy minimization performed using the OPLS_2005 force field (Schrödinger, LLC, New York, NY, 2022–4).

2.4. Molecular docking study and validation of docking

The molecular docking study was performed using the Glide module of Schrödinger, which utilizes the Emodel scoring function to choose among protein–ligand complexes for a specific ligand, and the GlideScore function to rank compounds, distinguishing those that bind strongly (actives) from those that do not (inactives) (Friesner et al., 2004, 2006; Halgren et al., 2004). Dulcitol and the five standard HDAC inhibitors were first docked with the HDAC8 grid using

the Glide XP module. The molecules that achieved XPGS ≤ -9 kcal/mol were further docked into HDAC1, HDAC2, HDAC3, HDAC4 and HDAC6 using Glide XP (Friesner et al., 2006) to predict their binding affinities and isoform selectivity. The docking protocol was validated by computing the root mean square deviation (RMSD) (Taha et al., 2011). The details of validation of the docked proteins are outlined in our prior studies (Sarkar et al., 2024).

2.5. In silico ADMET filtration

ADMET profiling is a crucial step in drug discovery as it streamlines the drug development process and accelerates the drug advancement journey by saving time, cost and unavoidable failures. SwissADME web application (`http://www.swissadme.ch/`) was used to predict potential pharmacokinetic properties such as absorption, distribution, metabolism and excretion (ADME) (Daina et al., 2017) while ProTox-II online tool (`https://tox-new.charite.de/protox_II/`) (Banerjee et al., 2018) and pKCSM web application (`https://biosig.lab.uq.edu.au/pkcsm/prediction`) (Pires et al., 2015) were utilized to evaluate the potential *in silico* toxicity of drug candidates, assessing factors such as lethal dose 50 (LD_{50}) value, hepatotoxicity, mutagenicity, carcinogenicity, immunogenicity, cytotoxicity, and overall toxicity class.

2.6. In silico prediction of cell line cytotoxicity

The potential cytotoxicity of the best hit was assessed using Cell Line Cytotoxicity Prediction (CLC-Pred 2.0) in the Way2Drug portal (`https://www.way2drug.com/clc-pred/`) (Lagunin et al., 2023). The chemical structures were imported in SMILES format, and the resulting output provided a probability score indicating the likelihood of the compound being active (Pa) or inactive (Pi) against various cancer cell lines.

2.7. Molecular dynamics simulation study

The stability and dynamic behavior of the best hit was evaluated individually with HDAC2, HDAC3 and HDAC8 by molecular dynamics simulation using Desmond (D. E. Shaw Research, New York, NY, 2022–4). The complexes underwent preliminary processing with the help of the Protein Preparation Wizard, which included complex optimization and minimization. The complexes were solvated using the simple point charge (SPC) water model (Mark and Nilsson, 2001) within orthorhombic boundary conditions followed by neutralization at a salt concentration of 0.15 mol/L using Na^+ and Cl^- ions (Jorgensen et al., 1983). Using the OPLS_2005 force field (Bowers et al., 2006), the solvated complex models were relaxed and subjected to MD simulation for 100 ns using the NPT ensemble at 310 K temperature and 1 bar pressure. The stability of simulation was examined by analysing RMSD, RMSF, radius of gyration (Rg), hydrogen bonds, and protein–ligand contacts of the protein and ligand over time.

3. Results and discussion

Cervical cancer is characterized by the substantial overexpression of HDAC2 (Huang et al., 2005; Lin et al., 2009), HDAC3 (Zhang et al., 2016; Sun et al., 2022) and HDAC8 (Vanaja et al., 2018). Therefore, the present *in silico* study was designed to evaluate the regulatory role of dulcitol targeting and inhibiting HDACs that are overexpressed in cervical cancer. The goal of this strategy was to facilitate the development of more effective drugs for the treatment of cervical cancer, offering a potential pathway to improved management and therapeutic outcomes for patients.

3.1. Molecular docking analysis

Dulcitol and the five standard HDAC inhibitors were initially docked with HDAC8 grid to predict the possible binding interactions between them. The highest binding affinity recorded for HDAC8 among the standard FDA-approved inhibitors was –9.882 kcal/mol. The binding affinities obtained from the molecular docking study revealed that dulcitol surpassed this benchmark, indicating that it could potentially serve as more effective HDAC8 inhibitor than the current standard drugs. Dulcitol was then further docked with other HDAC isoforms to predict its respective binding affinities. The validated structures of all HDACs (HDAC1, 2, 3, 4, 6 and 8) were used from our prior studies (Sarkar et al., 2024; Debnath et al., 2019). Dulcitol stood out due to its remarkable binding affinities not only for HDAC8 but also for HDAC2 and HDAC3.

The binding affinity of dulcitol for HDAC2 was –10.172 Kcal/mol, for HDAC3 was –10.683 Kcal/mol and for HDAC8 was –9.689 Kcal/mol. These values exceeded the highest binding affinities recorded for the standard HDAC inhibitors, which were –9.939 Kcal/mol for HDAC2, –8.532 Kcal/mol for HDAC3 and –9.882 Kcal/mol for HDAC8. This suggests that dulcitol might have a broad-spectrum inhibitory effect across the target HDAC isoforms.

The docking scores of dulcitol and the standard HDAC inhibitors against all the HDAC isoforms are provided in Table 1. The fact that dulcitol exhibited higher binding affinities than all standard FDA-approved HDAC inhibitors for HDAC2, HDAC3 and HDAC8, underscores its potential as a more potent multi-targeted inhibitor.

Interestingly, when docked with other off-target HDAC isoforms, dulcitol exhibited significantly lower binding affinities for HDAC1, HDAC4, and HDAC6, indicating that it was less likely to inhibit these off-target HDACs. This selectivity was crucial because it reduced the likelihood of off-target effects, which could otherwise lead to unwanted side effects. Therefore, the ability of dulcitol to selectively inhibit HDAC2, HDAC3, and HDAC8, while sparing other HDAC isoforms, presented a significant advantage in developing multi-targeted epigenetic therapies for diseases like cervical cancer, where these specific HDACs are notably overexpressed.

HDAC2 consists of a highly conserved catalytic domain containing a lipophilic tube followed by a deep catalytic site housing its Zn^{2+} cofactor as well as an internal 'foot pocket' (Haberland and Henning, 2009). The hydrophobic tube that joins the opening rim to the catalytic site is composed of GLY-154, PHE-155, HIS-183, PHE-210 and LEU-276 residues (Bressi et al., 2010; Hou et al., 2011). The catalytic site is composed of HIS-145, HIS-146,

Table 1: Docking score of dulcitol and the standard HDAC inhibitors against different HDAC isoforms

Name	HDAC2	HDAC3	HDAC8	HDAC1	HDAC4	HDAC6
Dulcitol	–10.172	–10.683	–9.689	–5.475	–8.907	–5.412
Panobinostat	–8.812	–8.532	–9.882	–8.548	–8.168	–3.397
Vorinostat	–9.939	–7.584	–9.179	–8.272	–6.967	–2.535
Pracinostat	–8.357	–8.778	–8.976	–8.306	–7.587	–4.318
Belinostat	–6.568	–4.673	–7.812	–5.689	–7.936	–4.032
Romidepsin	–4.040	–4.704	–1.969	–4.425	–2.809	–3.231

TYR-308, ASP-181, HIS-183, and ASP-269, while residues like TYR-29, MET-35, ARG-39, PHE-114, and LEU-144 comprise the internal foot pocket (Bressi et al., 2010; Hou et al., 2011; Zhou et al., 2017). Interactions with these key residues within the HDAC2 catalytic domain in different combinations play crucial role in HDAC2 inhibition (Tateing and Suree, 2022). The docking analysis of dulcitol with HDAC2 showed that the majority of the hydrogen bonds occurred with GLY-154 and GLY-143. Conventional hydrogen bond was predominant in the interaction between dulcitol and GLY-154 and GLY-143 residues of HDAC2. The hydroxyl group of dulcitol interacted with the Zn^{2+} ion in the active site of HDAC2 pocket (Fig. 1(a)).

The active site of HDAC3 was situated between dimer A and C. The residues involved in interactions with HDAC3 were HIS-17, ALA-20, GLY-21, HIS-22, LYS-25, ARG-265, VAL-300, ARG-301, and TYR-331 in dimer A, and LYS-449, TYR-470, TYR-471, LYS-474, and LYS-475 in dimer C (Watson et al., 2012). The docking analysis of dulcitol with HDAC3 showed that the majority of the hydrogen bonds occurred with TYR-298, GLY-143 and HIS-135. The hydroxyl group of dulcitol interacted with the Zn^{2+} ion in the active site of HDAC3 pocket (Fig. 1(b)).

On the other hand, the HDAC8 active site consists of two pockets, one immediately adjacent to another. The first catalytic pocket consists of a long, narrow, hydrophobic tunnel leading to a cavity where its Zn^{2+} cofactor is located. The tunnel measures about 11 Å and while it is formed by PHE-152, PHE-208, HIS-180, GLY-151, MET-274 and TYR-306, the Zn^{2+} binding area is formed by HIS-142, HIS-143, TYR-306. The second pocket measures about 14 Å and is lined by ARG-37, TYR-100, TYR-111, PHE-152 and TYR-306 (Somoza et al., 2004; Sarkar et al., 2024). In this study, the docking analysis of dulcitol with HDAC8 showed that the majority of the hydrogen bonds occurred with HIS-142 and HIS-143 which indicated that most of the hits bind to the catalytic pocket of HDAC8. The hydroxyl group of dulcitol interacted with the Zn^{2+} ion in the active site of HDAC8 (Fig. 1(c)).

Therefore, the protein–ligand interaction analyses revealed that dulcitol interacted with crucial amino acid residues and the Zn^{2+} ion present in the active site of all the target histone deacetylases (HDAC2, HDAC3, and HDAC8) which, in turn, indicates its potential affinity for these target receptors. The intermolecular interactions of dulcitol with HDAC2, HDAC3 and HDAC8 are represented in Fig. 1.

The docking analysis of the standard HDAC inhibitors with HDAC2 revealed that most of the inhibitors, amidst other additional interactions, notably formed hydrogen bonds with

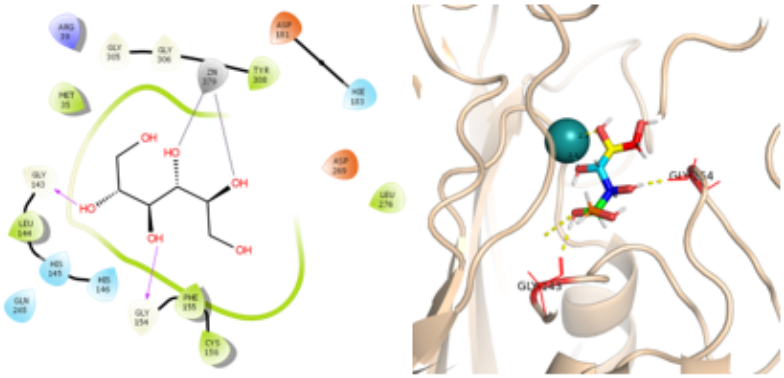

(a)

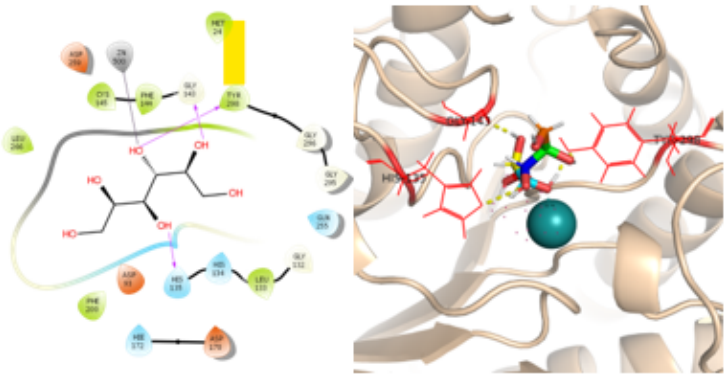

(b)

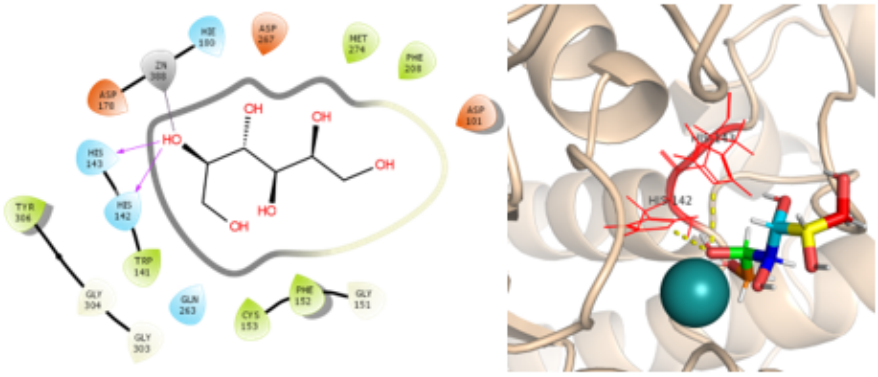

(c)

Figure 1: 2D (left) and 3D (right) ligand interaction diagram of dulcitol with (a) HDAC2 (b) HDAC3 (c) HDAC8 In 2D, hydrogen bonds are shown as purple lines, pi–pi interactions are shown in green lines and coordination of the zinc ion as black lines. In 3D, side chains of active site residues are shown as red wires and ligand as spectrum stick. The zinc ion is depicted as cyan ball. Hydrogen bonds are shown as yellow dashed lines and coordination of the zinc ion as cyan–dashed lines.

GLY-154 and interacted with Zn^{2+} ion, both of which are located in the active site of HDAC2. Similarly, for HDAC3, the standard inhibitors formed a metal coordination bond with the Zn^{2+} ion and a hydrogen bond with GLY-143, which are part of the HDAC3 active site. Additionally, most standard HDAC inhibitors interacted with the Zn^{2+} ion and the amino acid residues HIS-142 and HIS-143 through hydrogen bonds, in addition to other interactions, in case of HDAC8. These interactions of the known standard HDAC inhibitors with the target HDACs align with those observed in case of the selected hit, dulcitol, reinforcing its potential as a multi-target inhibitor of HDAC2, HDAC3, and HDAC8. The 2D protein-ligand interaction diagram of all the standard HDAC inhibitors with HDAC2, HDAC3 and HDAC8 are provided in Fig.2 - Fig 4.

3.2. In silico ADMET analysis

The ADMET prediction was carried out to assess the absorption, distribution, metabolism, excretion and toxicity of dulcitol. For a drug to be effective, it must be well-absorbed, properly distributed to its target, metabolized in a way that enhances its activity, and excreted safely without causing harm (Zrieq et al., 2021). According to the ADMET results, dulcitol passed all the ADME criteria except for the GI absorption, which could be optimized through appropriate drug delivery vehicle and/or via structural modification. In addition, in silico toxicity prediction revealed dulcitol as a "non–toxic" with an LD50 value of 13,500 mg/kg with no active hepatotoxicity, carcinogenicity, mutagenicity, immunogenecity and cytotoxicity. Additionally, dulcitol showed negative results in the AMES mutagenesis test, indicating it is not mutagenic. It also demonstrated no inhibition of the human ether-a-go-go related gene (hERG), which is associated with cardiac toxicity, and did not cause skin sensitization. These findings highlight the overall safety profile of dulcitol, positioning it as a highly promising lead compound for further drug development. An overview of the physicochemical properties, drug-likeness, pharmacokinetics, and toxicity properties of dulcitol, along with a bioavailability radar, are summarized in Table 2.

Table 2: Physicochemical properties, drug–likeness, bioavailability, pharmacokinetics and toxicity parameters of dulcitol

Physicochemical properties	**Dulcitol**
Molecular weight (g/mol)	182.17
Number of heavy atoms	12
Number of aromatic heavy atoms	0
Fraction Csp3	1.00
Number of rotatable bonds	5
Number of H–bond acceptors	6
Number of H–bond donors	6
Molar refractivity	37.93
TPSA ($Å^2$)	121.38

Continued on next page

Physicochemical properties	Dulcitol
Drug likeness	
Lipinski	Yes
Veber	Yes
Egan	Yes
Bioavailability score	0.55
Bioavailability radar	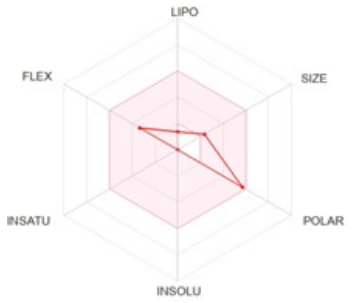
Pharmacokinetics	
GI absorption	Low
BBB permeability	No
CYP1A2 inhibitor	No
CYP2C19 inhibitor	No
CYP2C9 inhibitor	No
CYP2D6 inhibitor	No
CYP3A4 inhibitor	No
Toxicity	
AMES toxicity	No
hERG I inhibitor	No
hERG II inhibitor	No
Skin sensitization	No
Hepatotoxicity	No
Carcinogenecity	No
Mutagenicity	No
Immunogenecity	No
Cytotoxicity	No
Toxicity class	6 (Non toxic)
LD50 value (mg/kg)	13500

TPSA: Topological polar surface area, AMES: Salmonella/microsome mutagenicity assay, hERG: human ether–a–go–go–related gene, LD50: Lethal dose 50

3.3. In silico prediction of cell line cytotoxicity

The cytotoxicity of selected hit, dulcitol was assessed by predicting its Pa and Pi values against cancer cell lines. The results indicated that dulcitol exhibited significant cytotoxicity against

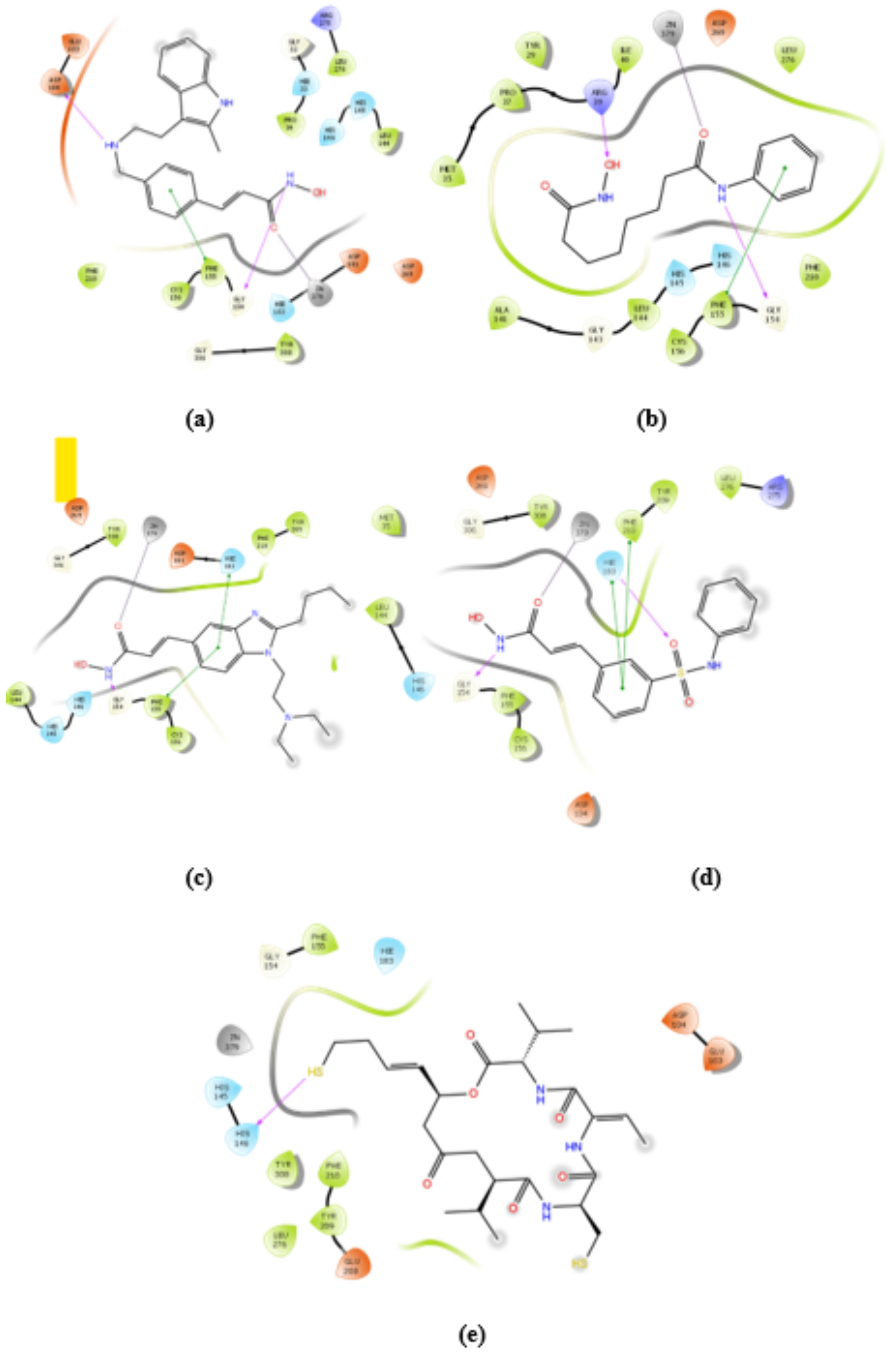

Figure 2: 2D protein–ligand interaction of HDAC2 and (a) Panobinostat (b) Vorinostat (c) Pracinostat (d) Belinostat (e) Romidepsin

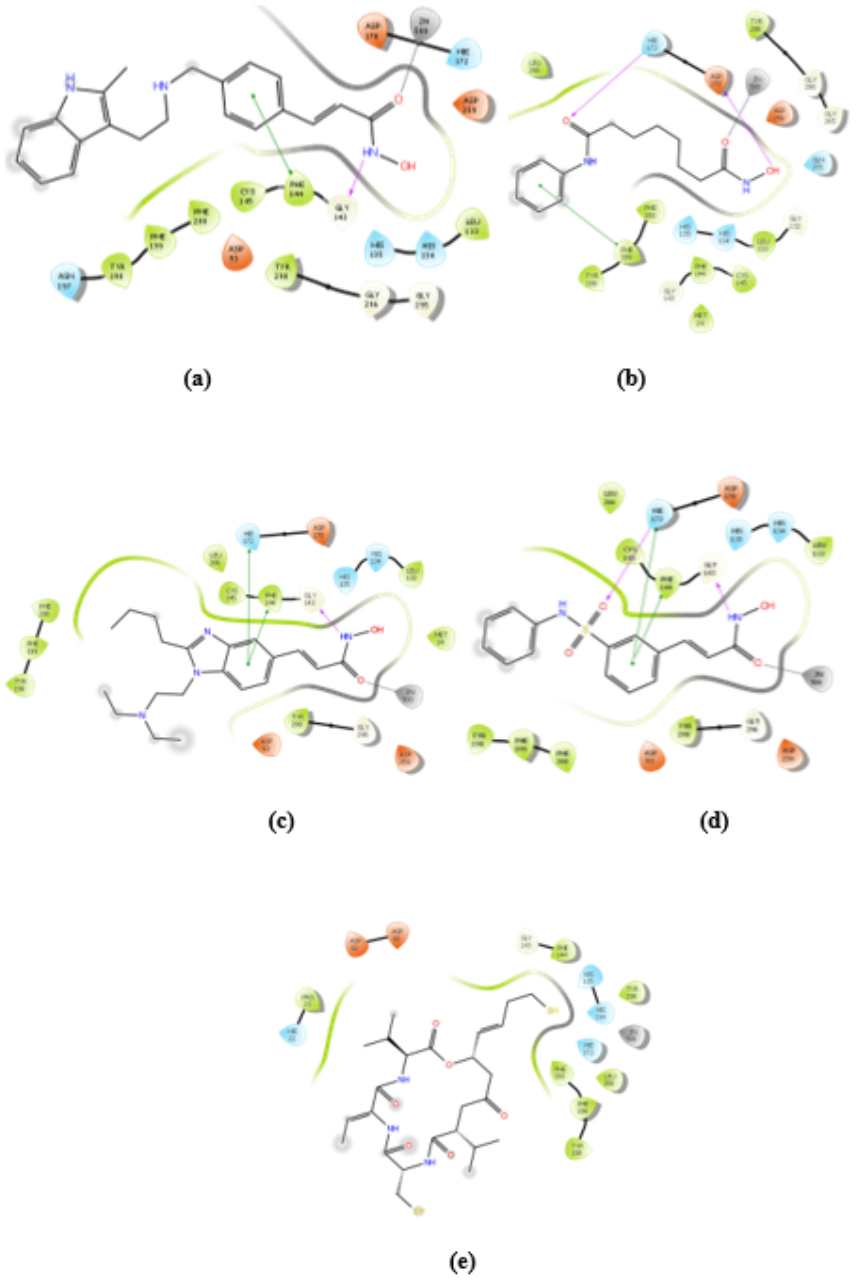

Figure 3: 2D protein–ligand interaction of HDAC3 and (a) Panobinostat (b) Vorinostat (c) Pracinostat (d) Belinostat (e) Romidepsin

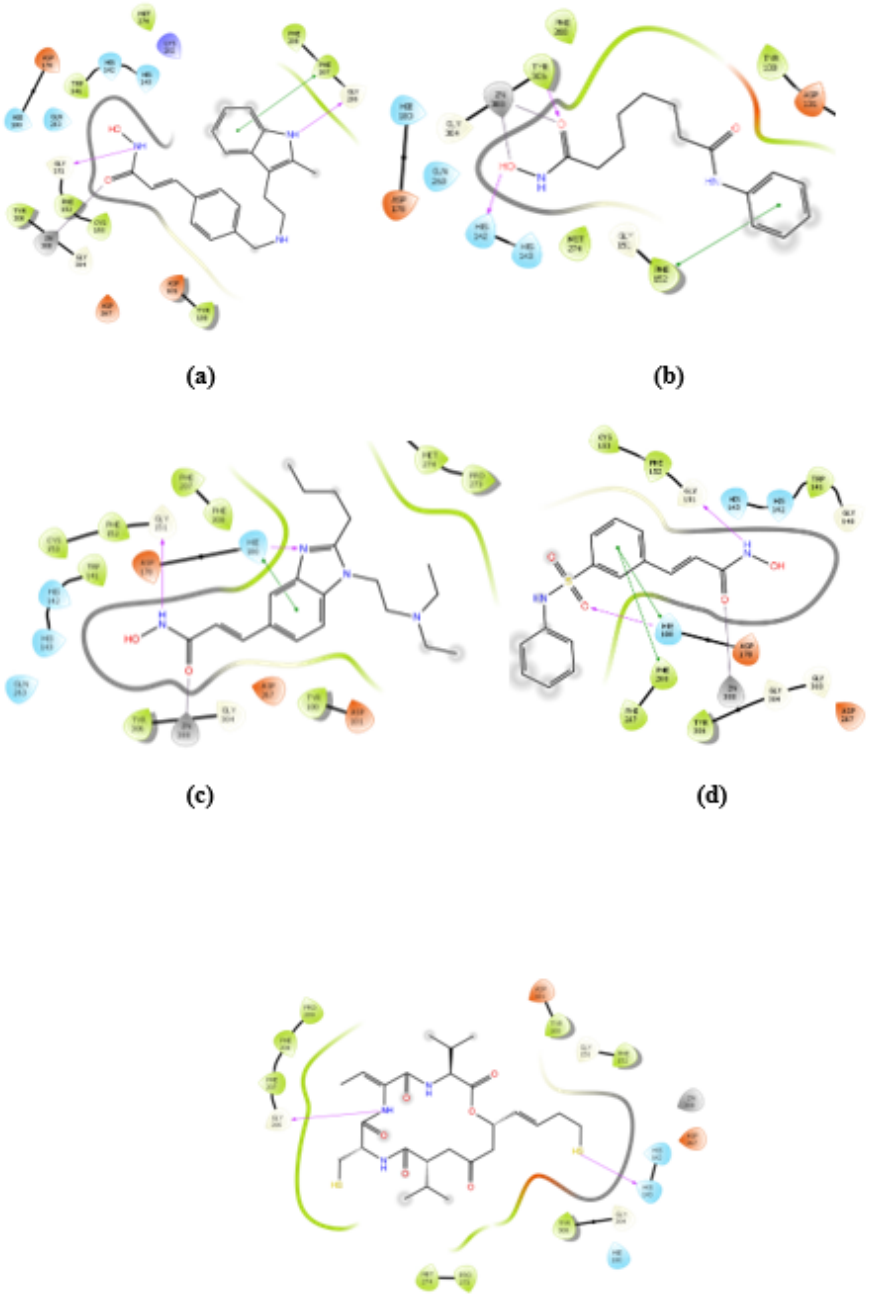

Figure 4: 2D protein–ligand interaction of HDAC8 and (a) Panobinostat (b) Vorinostat (c) Pracinostat (d) Belinostat (e) Romidepsin

multiple cancer cell lines with Pa values greater than 0.5 which in turn, underscores dulcitol's potential as a potent anti-cancer agent. The prediction of cell line cytotoxicity of dulcitol for cancer cells (Pa $>$ 0.5) is shown in Table 3.

Table 3: In silico cytotoxicity prediction of dulcitol on cancer cell line by CLC–pred

Name	Cell line	Cell line full name	Tissue	Tumor type	Pa	Pi
Dulcitol	SN12C	Renal carcinoma	Kidney	Carcinoma	0.921	0.003
	UACC–62	Melanoma	Skin	Melanoma	0.916	0.003
	SF–539	Glioblastoma	Brain	Glioblastoma	0.916	0.004
	HOP–62	Non–small cell lung carcinoma	Lung	Carcinoma	0.909	0.004
	OVCAR–3	Ovarian adenocarcinoma	Ovarium	Adenocarcinoma	0.819	0.005
	HCT–116	Colon carcinoma	Colon	Carcinoma	0.812	0.005
	DU–145	Prostate carcinoma	Prostate	Carcinoma	0.782	0.006
	MCF7	Breast carcinoma	Breast	Carcinoma	0.777	0.012
	SF–268	Glioblastoma	Brain	Glioblastoma	0.730	0.005
	Hs 683	Oligodendroglioma	Brain	Glioma	0.613	0.023
	A2058	Melanoma	Skin	Melanoma	0.554	0.005
	HCT–15	Colon adenocarcinoma	Colon	Adenocarcinoma	0.555	0.015
	SK–OV–3	Ovarian carcinoma	Ovarium	Carcinoma	0.540	0.017
	OVCAR–5	Ovarian adenocarcinoma	Ovarium	Adenocarcinoma	0.514	0.021
	OVCAR–4	Ovarian adenocarcinoma	Ovarium	Adenocarcinoma	0.511	0.019

Overall, molecular docking, ADMET analysis and in silico prediction of cytotoxicity for dulcitol revealed a promising profile. Although poor GI absorption remained a limiting factor, it could be optimized through the use of appropriate drug delivery systems. Nonetheless, the absence of mutagenic, hepatotoxic, carcinogenic, immunogenic, and cytotoxic effects positioned dulcitol as a potentially safe therapeutic candidate which was subsequently subjected to molecular dynamics (MD) simulation studies to assess its stability and flexibility within biological systems.

3.4. Molecular dynamics simulation analysis

Molecular dynamics (MD) simulations were conducted to assess the stability of the bound conformation of the best hit within the binding cavities of HDAC2, HDAC3, and HDAC8 metalloproteins. To evaluate the conformational stability and flexibility of the dulcitol–HDAC2, HDAC3, and HDAC8 complexes, the systems were simulated for 100 ns. From the simulation trajectories, thermodynamic parameters such as root mean square deviation (RMSD),

root mean square fluctuation (RMSF), radius of gyration (Rg), hydrogen bonds (H-bonds), and protein-ligand contacts were generated.

The stability of the systems was investigated by computing their RMSD from the 100 ns MD simulation trajectories. The RMSD evaluates the deviations of the Cα atoms of the residues, thus reflecting the stability of the protein-ligand system. The protein Cα RMSD values of apo-proteins and that of the protein-ligand complexes were calculated from the MD simulation trajectories and plotted against time (Fig.5). It was observed that the average RMSD values of the Cα atoms of the apo-proteins HDAC2, HDAC3 and HDAC8 were 1.43 Å, 1.80 Å and 1.70 Å respectively. In contrast, the average RMSD values of dulcitol bound to HDAC2, HDAC3 and HDAC8 were 3.55 Å, 2.04 Å and 2.33 Å respectively. Both the protein RMSD and ligand RMSD for all the three targeted HDACs thus exhibited deviations close to 3.00 Å, which signify good convergence and stable conformation.

For HDAC2-dulcitol complex, the protein RMSD started around 0.3 Å at the beginning of the simulation, and gradually increased, stabilizing around 2.01 Å after about 20 ns. The protein RMSD appeared to be fairly consistent, fluctuating between 0.86 Å and 2.73 Å, indicating that the protein structure was relatively stable with minor conformational adjustments during the simulation. The ligand RMSD stabilized around 3.55 Å, with some fluctuations which suggested that upon binding, dulcitol underwent some movement to accommodate itself within the active site of the HDAC2 protein, though does not appear to completely unbind or move out of the binding pocket.

For HDAC3-dulcitol complex, both the protein and ligand RMSD values stabilized after the initial equilibration phase, indicating that the complex was stable throughout the simulation. The low and stable RMSD values for both HDAC3 (1.60 Å) and dulcitol (2.04 Å) suggested that upon binding to dulcitol, the HDAC3-dulcitol complex was stable and maintained its overall structure, reinforcing the reliability of the molecular docking results.

For HDAC8-dulcitol complex, the protein RMSD stabilized around 1.54 Å after about 20 ns. The ligand RMSD, on the other hand, exhibited some initial fluctuations up to 20 ns but eventually got stabilized around 2.74 Å with a dip in RMSD observed during the last 10 ns of the simulation. This decrease toward the end of the simulation might suggest a tighter binding conformation or a possible reorganization of dulcitol within the binding pocket of HDAC8. Therefore, investigating the HDAC-dulcitol complexes, it was observed that all the three complexes were quite stable and exhibited negligible alterations throughout the simulation in comparison to their corresponding free states. RMSF analysis provides significant insights into the behavior of individual amino acid residues within the protein, indicating the flexibility and movement of individual amino acid residues within a protein during molecular dynamics simulation. Higher the RMSF values, higher is the flexibility of the protein and hence stronger is the propensity of the amino acid residue of the protein to interact with the ligand. The Cα RMSF value of the ligand-protein complex system was calculated from 100 ns MD trajectory and plotted against residue number (Fig.6). In this study, the comparison between apo or unbound and dulcitol-bound states of HDAC2, HDAC3, and HDAC8 proteins revealed minimal differences in flexibility. As observed from Fig.6, the apo HDAC2 protein exhibited an average RMSF value of 0.827 Å while the system complexed with dulcitol presented an average value of 0.991

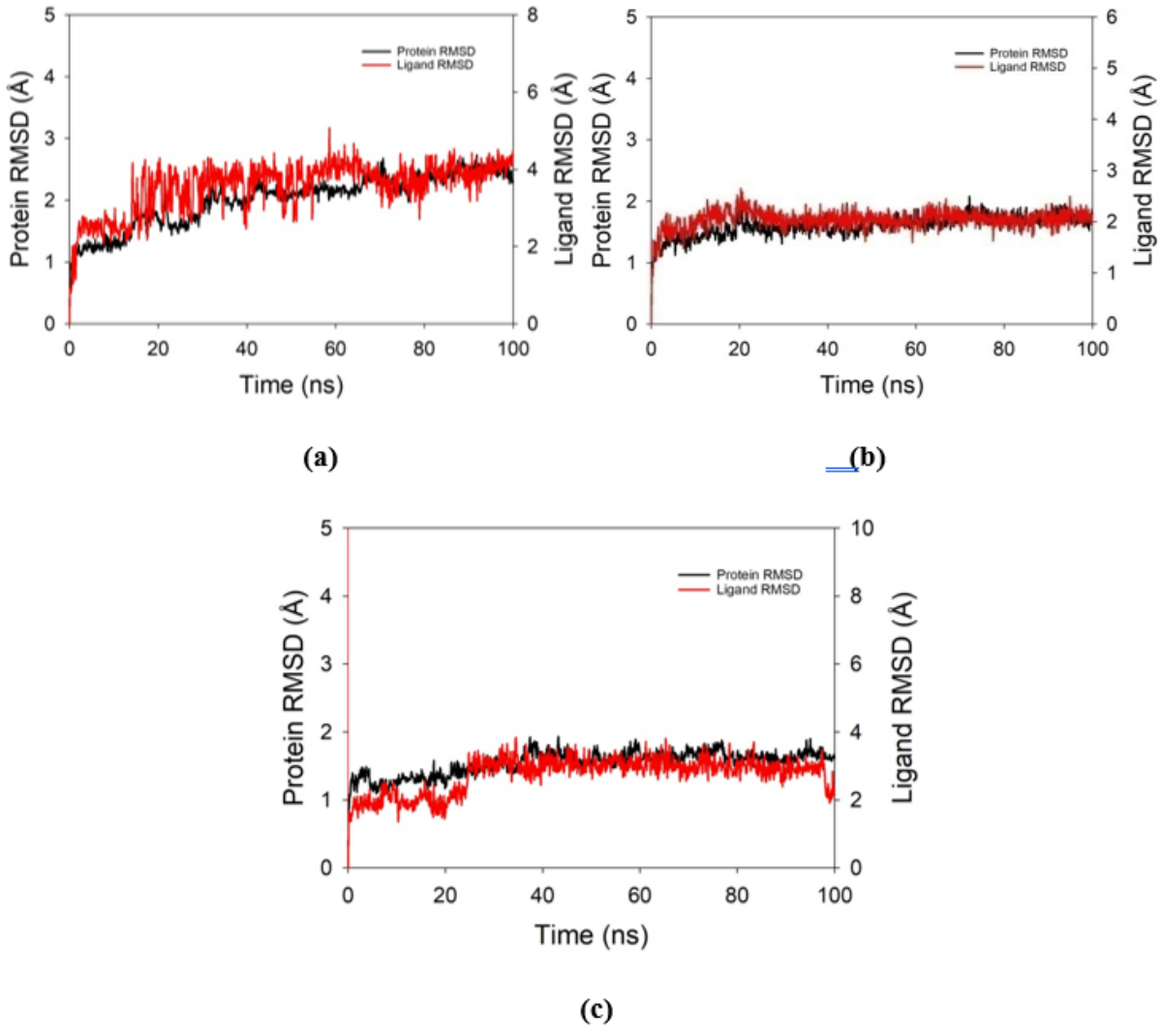

Figure 5: Time-dependent RMSD plots of $C\alpha$ atoms of (a) HDAC2-dulcitol (b) HDAC3-dulcitol and (c) HDAC8-dulcitol systems calculated from 100 ns MD simulation trajectories where protein RMSD is shown in black and RMSD of dulcitol is shown in red

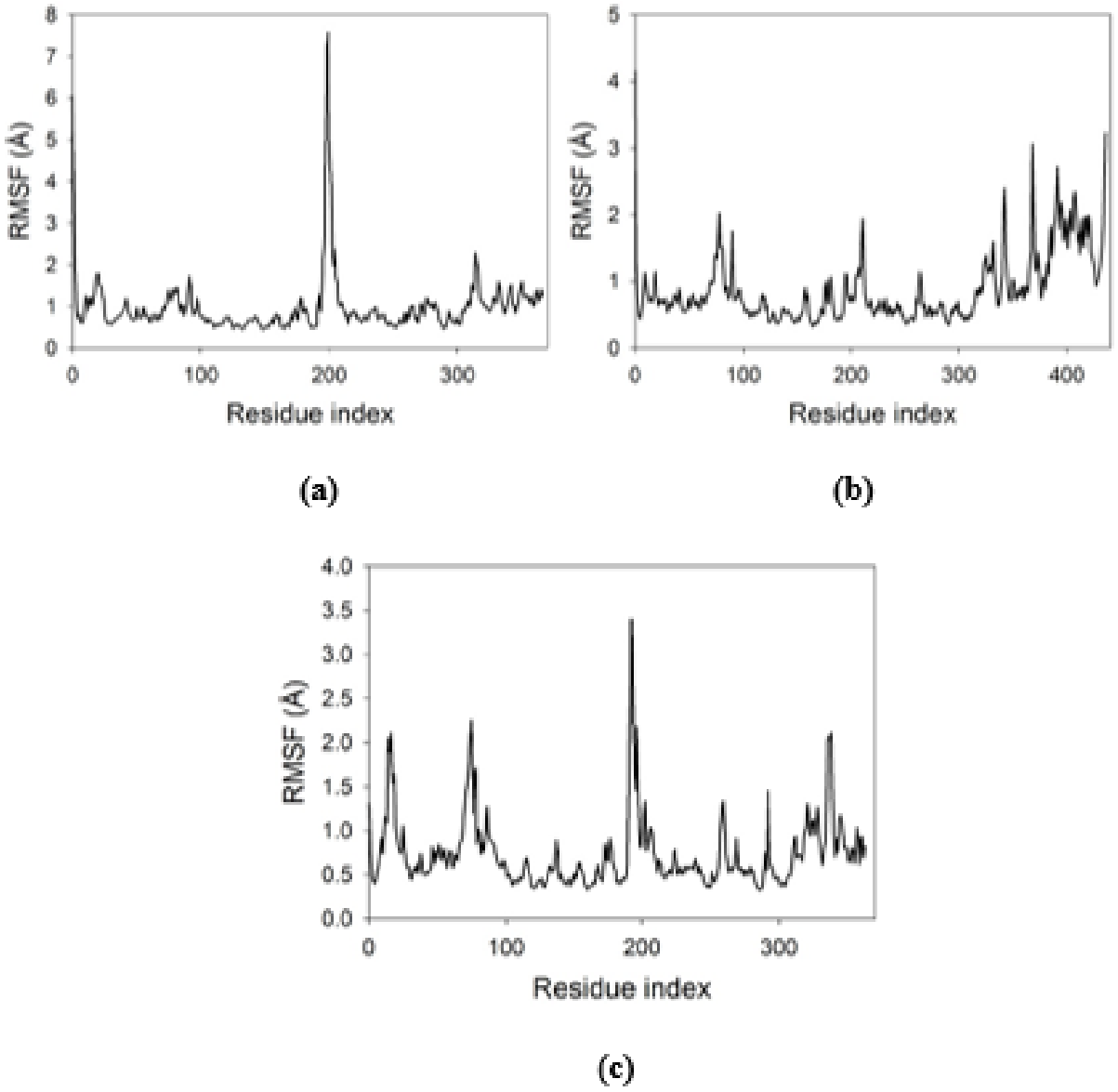

Figure 6: Protein RMSF calculated from 100 ns MD simulation trajectories for (a) HDAC2-dulcitol (b) HDAC3-dulcitol (c) HDAC8-dulcitol systems

Å. With HDAC3 protein system, the apo HDAC3 protein displayed an average RMSF of 0.900 Å while in complex with dulcitol, presented an average Rg of 0.878 Å. In case of HDAC8 protein system, the apo HDAC8 protein exhibited an average RMSF value of 0.771 Å while the system complexed with dulcitol presented an average value of 0.739 Å. Overall, these RMSF values suggested that the targeted proteins maintained more or less similar levels of flexibility in both their unbound and bound states. This could indicate that dulcitol binds in a way that stabilizes the targeted HDACs' existing structures without inducing major conformational changes or altering the flexibility of specific regions. The radius of gyration (Rg) plot further verified the stability of the ligand (dulcitol)-protein (HDAC2, HDAC3, and HDAC8) complexes. The Rg values were calculated and plotted over the 100 ns atomistic MD simulation trajectory (Fig.7). This parameter provides valuable information about the compactness of the proteins throughout

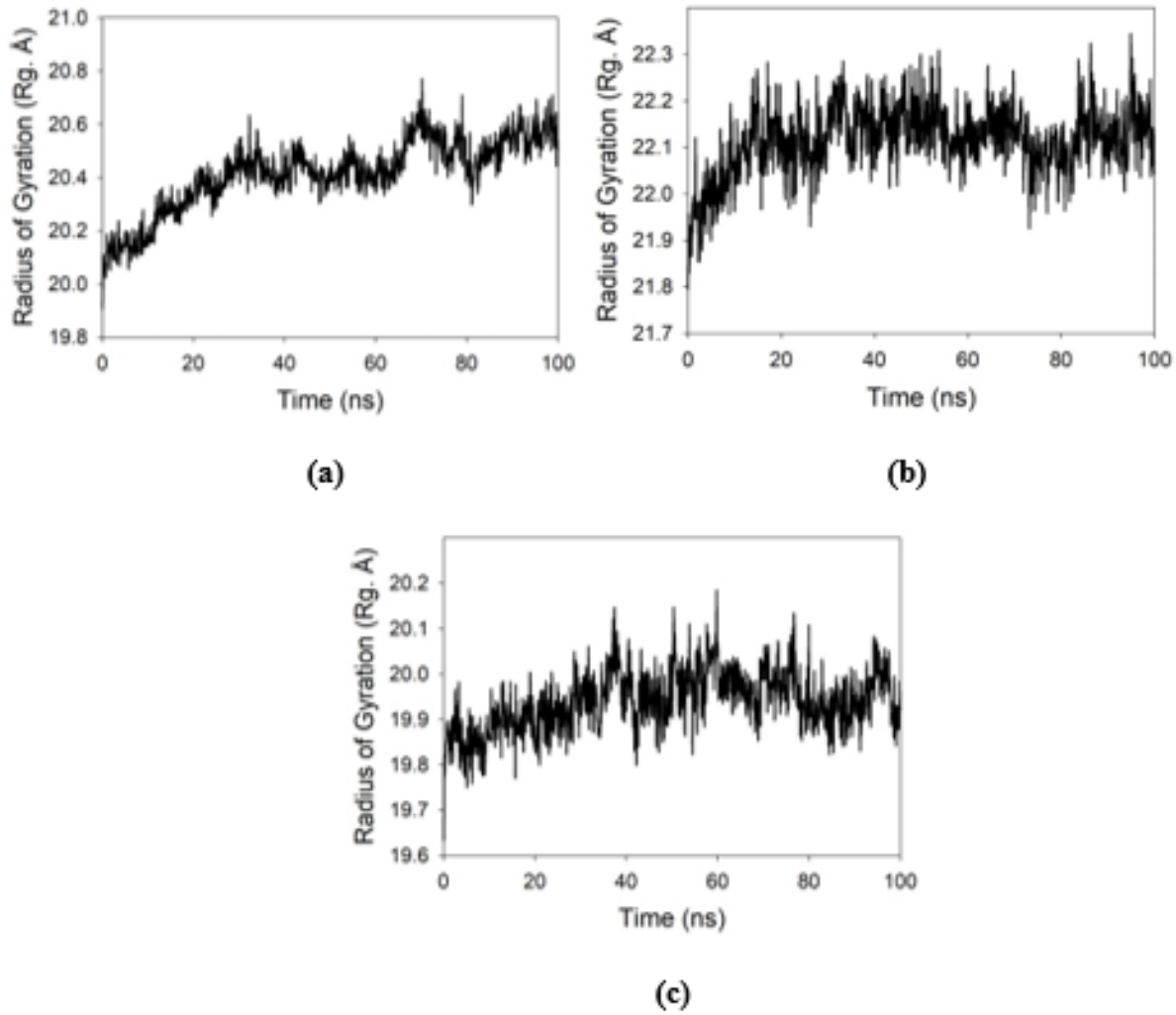

Figure 7: Radius of gyration (Rg) plots of $C\alpha$ atoms of (a) HDAC2-dulcitol (b) HDAC3-dulcitol (c) HDAC8-dulcitol systems calculated from 100 ns MD simulation trajectories

the simulation period. Higher Rg values correspond to less compact structures, while lower Rg values indicate more compact structures. According to the graphs, the apo-proteins HDAC2, HDAC3, and HDAC8 had average Rg values of 20.23 Å, 22.19 Å, and 19.99 Å, respectively. In contrast, the dulcitol-bound HDAC2, HDAC3, and HDAC8 complexes had average Rg values of 20.41 Å, 22.11 Å, and 19.94 Å, respectively. These values showed steady behavior of the targeted proteins throughout the simulation in both their unbound and dulcitol-bound forms. This suggested that the binding of dulcitol was likely favorable and did not cause the targeted HDACs to undergo large-scale folding or unfolding, thereby avoiding any significant destabilization of the protein structure. This stability further vouched for the effectiveness of dulcitol as a therapeutic agent, as it implied that the structure of the protein was maintained across the apo and ligand-bound states over the 100 ns simulation period for all the three target proteins HDAC2, HDAC3, and HDAC8. This study also performed an in-depth analysis of hydrogen bond formation within biomolecular systems. The analysis of hydrogen bond formation between the protein-ligand complexes over the 100 ns MD trajectory highlighted the significant role of hydrogen bonds in maintaining the stability and integrity of the complexes. The num-

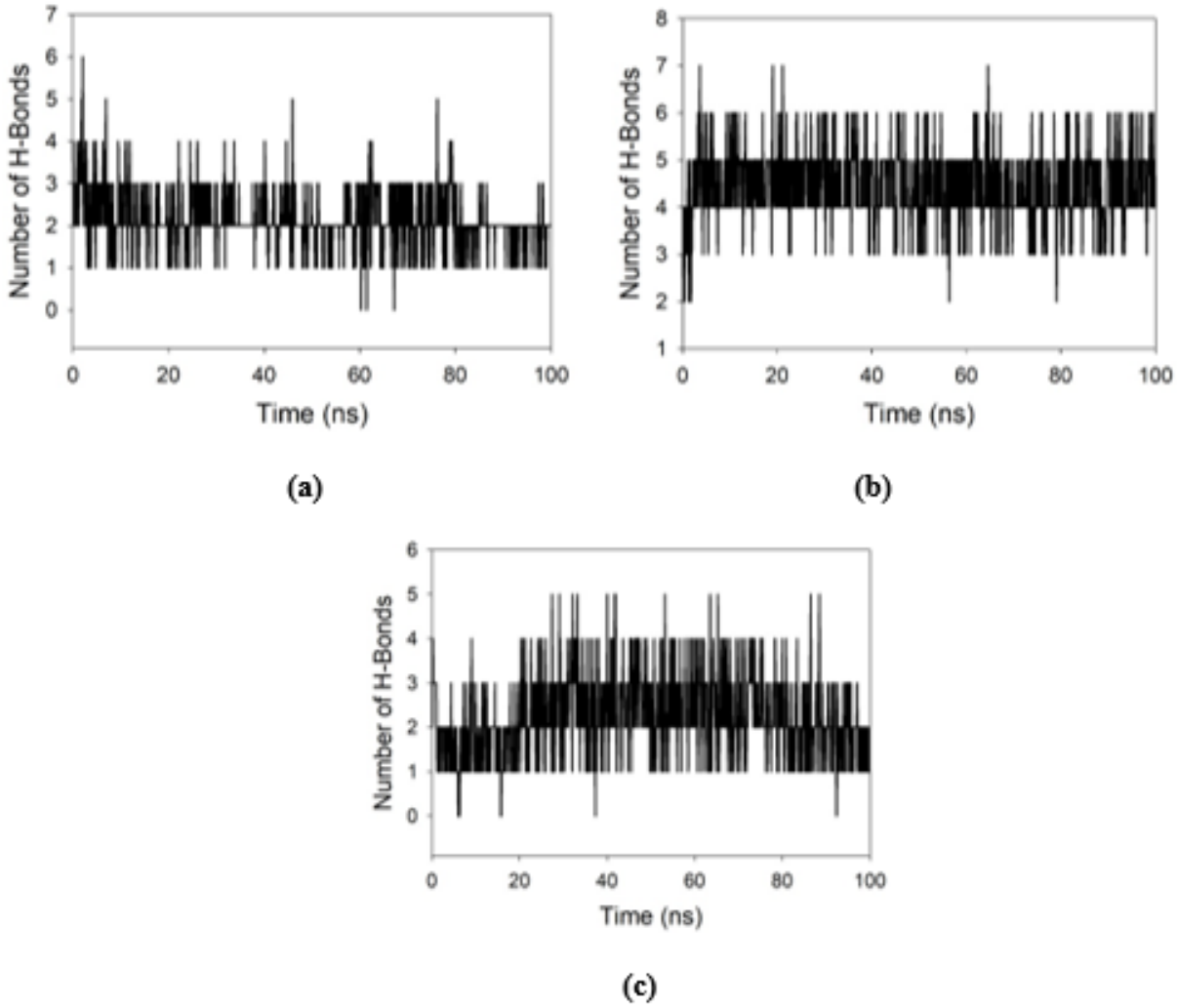

Figure 8: Formation of hydrogen bonds in (a) HDAC2-dulcitol (b) HDAC3-dulcitol (c) HDAC8-dulcitol systems

ber of hydrogen bonds formed between protein-ligand complexes was determined from a 100 ns MD trajectory and plotted over time (Fig.8). The hydrogen bonds between the protein and ligand signify substantial interaction and stability of the complex. For the dulcitol-HDAC2 and dulcitol-HDAC8 complexes, an average of two hydrogen bonds was consistently maintained throughout the simulation. Notably, the dulcitol-HDAC3 complex demonstrated even greater stability with the formation of four hydrogen bonds over the entire 100 ns. The steady hydrogen bond formation observed from 0 to 100 ns for all three HDAC-dulcitol complexes suggested that dulcitol remained consistently bound within the binding pockets of HDAC2, HDAC3, and HDAC8, aligning well with prior analyses regarding the stability, flexibility, and compactness of the systems. Having established the impact of dulcitol on the conformations and structural changes of the proteins, we aimed to uncover the events driving these changes by examining the protein-ligand interactions between dulcitol and the residues of the targeted HDACs during the simulation period. The protein-ligand interactions during the simulation were represented by stacked bar charts, categorized into hydrogen bonds, hydrophobic interactions, water bridges, and ionic interactions (Fig.9). For the dulcitol-HDAC2 complex, the simulation interaction di-

agram showed hydrogen bonds with GLY–154 (75%) and GLY–307 (90%), in line with the docking results. It also formed ionic interactions with ASP–181 (180%), HIS–183 (100%), ASP–269 (100%), and water bridge interactions with ASP–274 (70%). These interactions highlight the significance of hydrogen bonds, ionic interactions and water-bridge contacts in maintaining the integrity of the complex. In the dulcitol-HDAC3 complex, primary hydrogen bonds were with HIS–134 (110%), HIS–135 (60%), GLY–143 (90%), ASP–170 (90%), and TYR–298 (100%). It also formed ionic interactions with ASP–170 (210%), HIS–172 (100%), ASP–259 (110%), and water bridges with GLY–297 (60%). This interaction pattern confirmed the docking results, especially with HIS–135, GLY–143, and TYR–298, indicating that the predicted docking interactions were also well-maintained throughout the simulation. The simulation interaction diagram of dulcitol with HDAC8 displayed H–bonds with GLY–140 (90%), GLY–151 (30%), GLN–263 (40%) and GLY–305 (50%). Additionally, it also formed ionic interactions with ASP–178 (150%), HIS–180 (100%), ASP–267 (110%), GLY–303 (80%) and water bridge interactions with ARG–37 (30%). All these protein-ligand interactions illustrated that dulcitol formed consistent and stable interactions across all three HDAC complexes, particularly through hydrogen bonds and ionic interactions. Furthermore, Fig.10 shows dulcitol within the binding pockets of HDAC2, HDAC3 and HDAC8 at different timeframes throughout the 100 ns MD simulation indicating that dulcitol remained consistently bound within the active site of all the three target proteins throughout the simulation. The alignment with docking analyses, especially in critical residues, also confirmed the reliability of the initial docking studies and emphasized the significance of these interactions in ensuring the stability and efficacy of the protein-ligand complexes.

Taken together, all these findings suggested that dulcitol was stable and well-bound within the binding pockets of HDAC2, HDAC3, and HDAC8 throughout the entire period of simulation, contributing to its potential as a multi-targeted inhibitor and highlighting its novel avenue in epigenetic cancer therapy although further *in vitro* and *in vivo* studies are warranted.

4. Conclusion

The present study identified dulcitol as a promising multi-targeted inhibitor of HDAC2, HDAC3, and HDAC8, which are overexpressed in cervical cancer. Molecular docking and dynamics simulations demonstrated dulcitol's high binding affinity and stable interactions with these target HDACs as compared to standard FDA-approved HDAC inhibitors. The compound exhibited favorable ADMET properties and a good safety profile. The selectivity of dulcitol for the target HDACs over other isoforms suggested its potential for reduced off-target effects. However, further *in vitro* and *in vivo* studies are necessary to fully evaluate the efficacy and safety of dulcitol at cellular and molecular levels. Overall, this study paved the way for developing dulcitol as a new epi-therapeutic agent for treating cervical cancer.

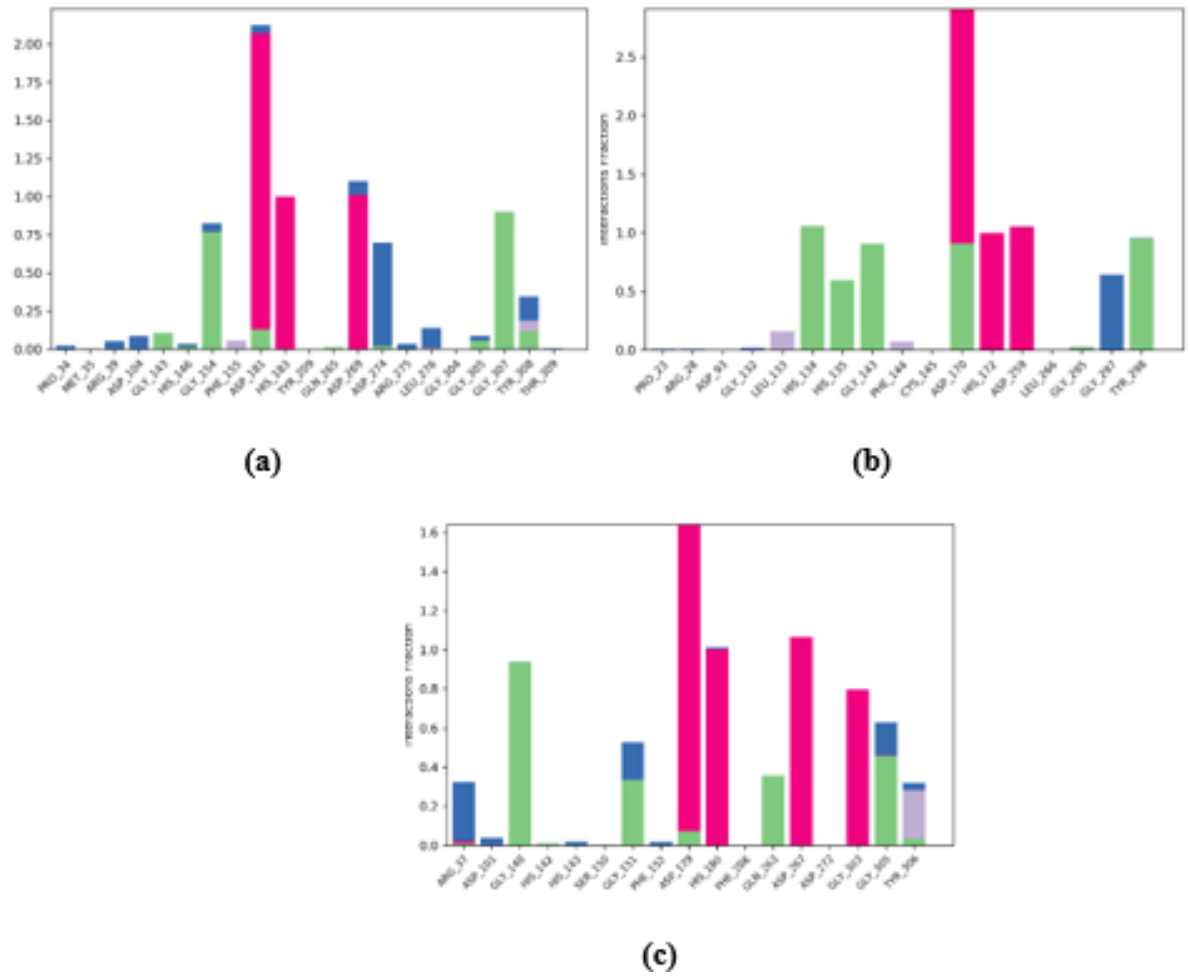

Figure 9: Protein-ligand contacts in (a) HDAC2-dulcitol (b) HDAC3-dulcitol (c) HDAC8-dulcitol systems

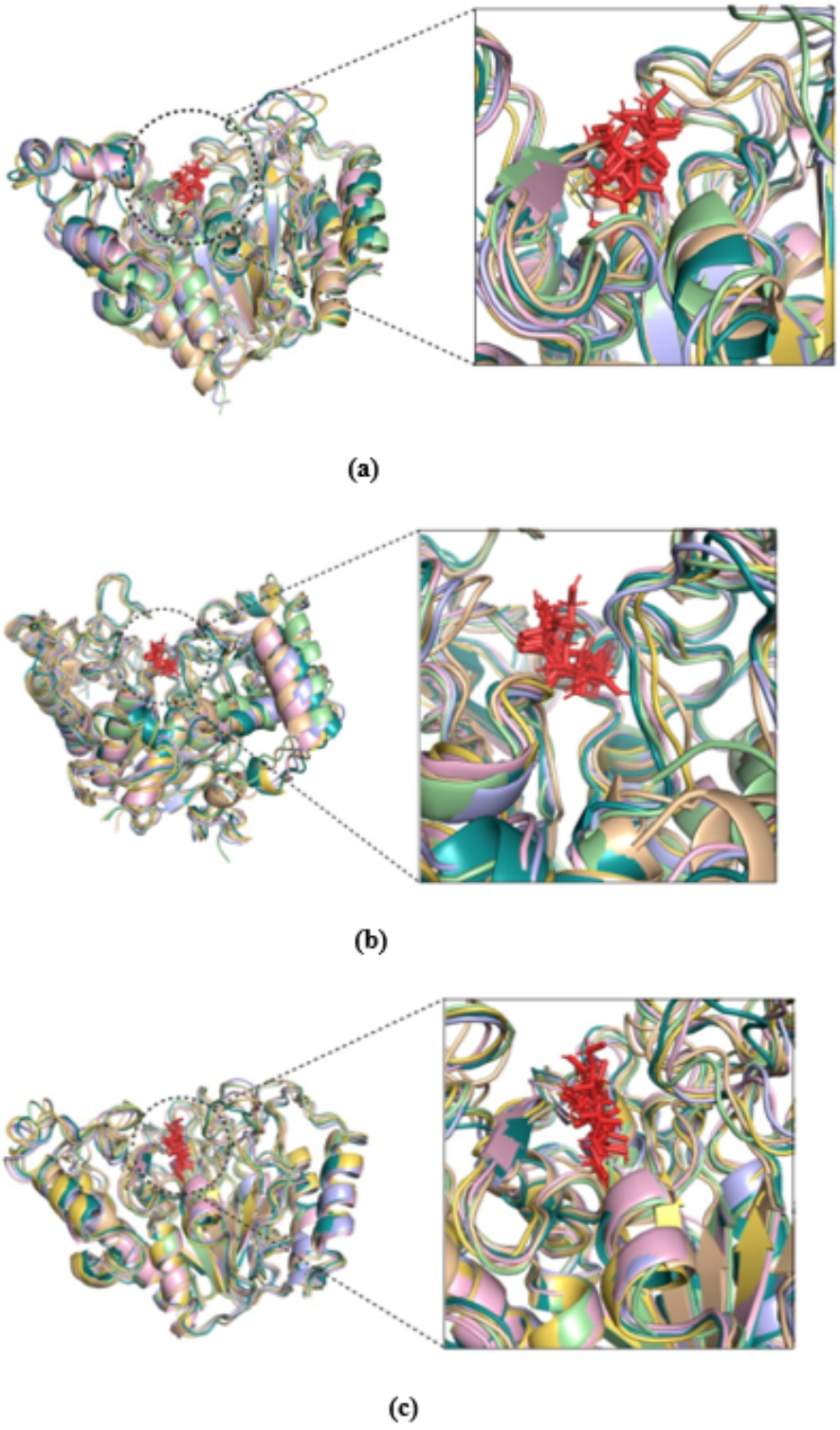

Figure 10: Superimposed snapshots of (a) HDAC2- (b) HDAC3- and (c) HDAC8- docked with dulcitol at different time frames of simulation (0 ns: wheat, 20 ns: pale green, 40 ns: light blue, 60 ns: light pink, 80 ns: yellow, 100 ns: deep teal)

Acknowledgments

Kakali Sarkar and Maria Debbarma are thankful to the Department of Science and Technology (DST), Govt. of India for providing INSPIRE fellowship (Ref. No. DST/INSPIRE Fellowship/IF210302 and DST/INSPIRE Fellowship/IF230470 respectively). The authors are thankful to Dr. Rajat Ghosh, Department of Pharmacy, Tripura University for providing Schrodinger software facilities and workstation. The authors are also thankful to Tripura University for providing library, internet, and infrastructural facilities.

Statements & Declarations

Funding

The authors did not receive support from any organization for the submitted work.

Competing Interests

The authors have no competing interests to declare that are relevant to the content of this article.

Ethics Approval

Not applicable.

Consent to Participate

Not applicable.

Consent to Publish

All authors consented to publish the article.

Availability of data and materials

All the data thus generated for this research work are included in the manuscript.

Author contributions

Conceptualization: Samir Kumar Sil and Kakali Sarkar; Methodology: Kakali Sarkar & Maria Debbarma; Formal analysis and investigation: Kakali Sarkar, Maria Debbarma and Aishi Chakraborty; Writing – original draft preparation: Kakali Sarkar; Writing – review and editing: Samir Kumar Sil and Sudhan Debnath; Supervision: Samir Kumar Sil.

References

Alseksek, R.K., Ramadan, W.S., Saleh, E., El-Awady, R., 2022. The role of hdacs in the response of cancer cells to cellular stress and the potential for therapeutic intervention. International Journal of Molecular Sciences 23, 8141. doi:10.3390/ijms23158141.

Banerjee, P., Eckert, A.O., Schrey, A.K., Preissner, R., 2018. Protox-ii: a webserver for the prediction of toxicity of chemicals. Nucleic Acids Research 46, W257–W263. doi:10.1093/nar/gky318.

Bottomley, M.J., Lo Surdo, P., Di Giovine, P., Cirillo, A., Scarpelli, R., Ferrigno, F., Jones, P., Neddermann, P., De Francesco, R., Steinkühler, C., Gallinari, P., Carfí, A., 2008. Structural and functional analysis of the human hdac4 catalytic domain reveals a regulatory structural zinc-binding domain. Journal of Biological Chemistry 283, 26694–26704. doi:10.1074/jbc.m803514200.

Bowers, K.J., Chow, E., Xu, H., Dror, R.O., Eastwood, M.P., Gregerson, B.A., Klepeis, J.L., Kolossváry, I., Moraes, M.A., Sacerdoti, F.D., Salmon, J.K., Shan, Y., Shaw, D.E., 2006. Molecular dynamics—scalable algorithms for molecular dynamics simulations on commodity clusters doi:10.1145/1188455.1188544.

Bressi, J.C., Jennings, A.J., Skene, R., Wu, Y., Melkus, R., De Jong, R., O'Connell, S., Grimshaw, C.E., Navre, M., Gangloff, A.R., 2010. Exploration of the hdac2 foot pocket: Synthesis and sar of substituted n-(2-aminophenyl)benzamides. Bioorganic & Medicinal Chemistry Letters 20, 3142–3145. doi:10.1016/j.bmcl.2010.03.091.

Daina, A., Michielin, O., Zoete, V., 2017. Swissadme: a free web tool to evaluate pharmacokinetics, drug-likeness and medicinal chemistry friendliness of small molecules. Scientific Reports 7. doi:10.1038/srep42717.

Debnath, S., Debnath, T., Bhaumik, S., Majumdar, S., Kalle, A.M., Aparna, V., 2019. Discovery of novel potential selective hdac8 inhibitors by combine ligand-based, structure-based virtual screening and in-vitro biological evaluation. Scientific Reports 9, 1–15. URL: https://doi.org/10.1038/s41598-019-53376-y, doi:10.1038/s41598-019-53376-y.

Erukainure, O.L., Chukwuma, C.I., Islam, M.S., 2019. Raffia palm (raphia hookeri) wine: Qualitative sugar profile, functional chemistry, and antidiabetic properties. Food Bioscience 30, 100423. doi:10.1016/j.fbio.2019.100423.

Friesner, R.A., Banks, J.L., Murphy, R.B., Halgren, T.A., Klicic, J.J., Mainz, D.T., Repasky, M.P., Knoll, E.H., Shelley, M., Perry, J.K., Shaw, D.E., Francis, P., Shenkin, P.S., 2004. GLIDE: A new approach for rapid, accurate docking and scoring. I. method and assessment of docking accuracy. Journal of Medicinal Chemistry 47, 1739–1749. doi:10.1021/jm0306430.

Friesner, R.A., Murphy, R.B., Repasky, M.P., Frye, L.L., Greenwood, J.R., Halgren, T.A., Sanschagrin, P.C., Mainz, D.T., 2006. Extra precision GLIDE: Docking and scoring incorporating a model of hydrophobic enclosure for protein–ligand complexes. Journal of Medicinal Chemistry 49, 6177–6196. doi:10.1021/jm051256o.

Haberland, J., Henning, M.A., 2009. The isolation number of a graph. Discrete Mathematics 309, 5569–5576. doi:10.1016/j.disc.2009.02.017.

Halgren, T.A., Murphy, R.B., Friesner, R.A., Beard, H.S., Frye, L.L., Pollard, W.T., Banks, J.L., 2004. GLIDE: A new approach for rapid, accurate docking and scoring. II. enrichment factors in database screening. Journal of Medicinal Chemistry 47, 1750–1759. doi:10.1021/jm030644s.

Harding, R.J., De Freitas, R.F., Collins, P., Franzoni, I., Ravichandran, M., Ouyang, H., Juarez-Ornelas, K.A., Lautens, M., Schapira, M., Von Delft, F., Santhakumar, V., Arrowsmith, C.H., 2017. Small molecule antagonists of the interaction between the histone deacetylase 6 zinc-finger domain and ubiquitin. Journal of Medicinal Chemistry 60, 9090–9096. doi:10.1021/acs.jmedchem.7b00933.

Hou, J., Feng, C., Li, Z., Fang, Q., Wang, H., Gu, G., Shi, Y., Liu, P., Xu, F., Yin, Z., Shen, J., Wang, P., 2011. Structure-based optimization of click-based histone deacetylase inhibitors. European Journal of Medicinal Chemistry 46, 3190–3200. doi:10.1016/j.ejmech.2011.04.027.

Hua, F.F., Xia, Y.H., Wu, D.P., Chen, R.X., Wang, Y.H., Pan, Y., Yang, J., Liang, W.F., 2012. Effect of down-regulation of histone deacetylase 2 protein expression on cell proliferation and cell cycle in cervical carcinoma. Chinese Medical Journal 41, 466–469. doi:10.3760/cma.j.issn.0529-5807.2012.07.008.

Huang, B.H., Laban, M., Leung, C.H., Lee, L., Lee, C.K., Salto-Tellez, M., Raju, G.C., Hooi, S.C., 2005. Inhibition of histone deacetylase 2 increases apoptosis and p21cip1/waf1 expression, independent of histone deacetylase 1. Cell Death and Differentiation 12, 395–404. doi:10.1038/sj.cdd.4401567.

Jorgensen, W.L., Chandrasekhar, J., Madura, J.D., Impey, R.W., Klein, M.L., 1983. Comparison of simple potential functions for simulating liquid water. The Journal of Chemical Physics 79, 926–935. doi:10.1063/1.445869.

Kobayashi, Y., Shen, J., Li, S.H., Kakizoe, E., Okunishi, H., Chen, J.F., 1997. Suppressive effects of a plant-origin polyol, dulcitol on collagen-induced arthritis in mice. Folia Pharmacologica Japonica 110, 132P–137P. doi:10.1254/fpj.110.supplement_132.

Lagunin, A.A., Rudik, A.V., Pogodin, P.V., Savosina, P.I., Tarasova, O.A., Dmitriev, A.V., Ivanov, S.M., Biziukova, N.Y., Druzhilovskiy, D.S., Filimonov, D.A., Poroikov, V.V., 2023. Clc-pred 2.0: a freely available web application for in silico prediction of human cell line

cytotoxicity and molecular mechanisms of action for druglike compounds. International Journal of Molecular Sciences 24, 1689. doi:10.3390/ijms24021689.

Li, Y., Seto, E., 2016. Hdacs and hdac inhibitors in cancer development and therapy. Cold Spring Harbor Perspectives in Medicine 6, a026831. doi:10.1101/cshperspect.a026831.

Lin, X.L., Li, K., Yang, Z., Chen, B., Zhang, T., 2020. Dulcitol suppresses proliferation and migration of hepatocellular carcinoma via regulating sirt1/p53 pathway. Phytomedicine 66, 153112. doi:10.1016/j.phymed.2019.153112.

Lin, Z., Bazzaro, M., Wang, M.C., Chan, K.C., Peng, S., Roden, R.B.S., 2009. Combination of proteasome and hdac inhibitors for uterine cervical cancer treatment. Clinical Cancer Research 15, 570–577. doi:10.1158/1078-0432.CCR-08-1813.

Mark, P., Nilsson, L., 2001. Structure and dynamics of the TIP3P, SPC, and SPC/E water models at 298 k. The Journal of Physical Chemistry A 105, 9954–9960. doi:10.1021/jp003020w.

Millard, C.J., Watson, P.J., Celardo, I., Gordiyenko, Y., Cowley, S.M., Robinson, C.V., Fairall, L., Schwabe, J.W.R., 2013. Class i hdacs share a common mechanism of regulation by inositol phosphates. Molecular Cell 51, 57–67. doi:10.1016/j.molcel.2013.05.020.

Pidugu, V.R., Yarla, N.S., Pedada, S.R., Kalle, A.M., Satya, A.K., 2016. Design and synthesis of novel hdac8 inhibitory 2,5-disubstituted-1,3,4-oxadiazoles containing glycine and alanine hybrids with anticancer activity. Bioorganic & Medicinal Chemistry 24, 5611–5617. doi:10.1016/j.bmc.2016.09.022.

Pires, D.E.V., Blundell, T.L., Ascher, D.B., 2015. Pkcsm: Predicting small-molecule pharmacokinetic and toxicity properties using graph-based signatures. Journal of Medicinal Chemistry 58, 4066–4072. doi:10.1021/acs.jmedchem.5b00104.

Sarkar, K., Debnath, S., Sen, D., Kar, S., Sil, S.K., 2024. Crucial structural understanding for selective hdac8 inhibition: Common pharmacophores, molecular docking, molecular dynamics, and zinc binder analysis of selective hdac8 inhibitors. Medicinal Chemistry 20. doi:10.2174/0115734064320232240709105228.

Sastry, G.M., Adzhigirey, M., Day, T., Annabhimoju, R., Sherman, W., 2013. Protein and ligand preparation: parameters, protocols, and influence on virtual screening enrichments. Journal of Computer-Aided Molecular Design 27, 221–234. doi:10.1007/s10822-013-9644-8.

Sha, F., Zheng, Y., Chen, J., Chen, K., Cao, F., Yan, M., Ouyang, P.D., 2018. Tagatose manufacture through bio-oxidation of galactitol derived from waste xylose mother liquor. Green Chemistry 20, 2382–2391. doi:10.1039/C8GC00091C.

Somoza, J.R., Skene, R.J., Katz, B.A., Mol, C., Ho, J.D., Jennings, A.J., Luong, C., Arvai, A., Buggy, J.J., Chi, E., Tang, J., Sang, B.C., Verner, E., Wynands, R., Leahy, E.M., Dougan, D.R., Snell, G., Navre, M., Knuth, M.W., Swanson, R.V., McRee, D.E., Tari, L.W., 2004. Structural snapshots of human hdac8 provide insights into the class i histone deacetylases. Structure 12, 1325–1334. doi:10.1016/j.str.2004.04.01.

Sun, H., Saeedi, P., Karuranga, S., et al., 2022. Idf diabetes atlas: Global, regional, and country-level diabetes prevalence estimates for 2021 and projections for 2045. Diabetes Research and Clinical Practice 183, 109119. doi:10.1016/j.diabres.2021.109119.

Taha, M.O., Habash, M., Al-Hadidi, Z., Al-Bakri, A., Younis, K., Sisan, S., 2011. Docking-based comparative intermolecular contacts analysis as new 3d-qsar concept. Journal of Chemical Information and Modeling 51, 647–669. doi:10.1021/ci100368t.

Tateing, S., Suree, N., 2022. Decoding molecular recognition of inhibitors targeting hdac2 via molecular dynamics simulations and configurational entropy estimation. PLoS ONE 17, e0273265. doi:10.1371/journal.pone.0273265.

Ungerstedt, J.S., Sowa, Y., Xu, W.S., Shao, Y., Dokmanovic, M., Perez, G., Ngo, L., Holmgren, A., Jiang, X., Marks, P.A., 2005. Role of thioredoxin in the response of normal and transformed cells to histone deacetylase inhibitors. Proceedings of the National Academy of Sciences 102, 673–678. doi:10.1073/pnas.0408732102.

Vanaja, G.R., Ramulu, H.G., Kalle, A.M., 2018. Overexpressed hdac8 in cervical cancer cells shows functional redundancy of tubulin deacetylation with hdac6. Cell Communication and Signaling 16. doi:10.1186/s12964-018-0231-4.

Vannini, A., Volpari, C., Filocamo, G., Casavola, E.C., Brunetti, M., Renzoni, D., Chakravarty, P., Paolini, C., De Francesco, R., Gallinari, P., Steinkühler, C., Di Marco, S., 2004. Crystal structure of a eukaryotic zinc-dependent histone deacetylase, human hdac8, complexed with a hydroxamic acid inhibitor. Proceedings of the National Academy of Sciences 101, 15064–15069. doi:10.1073/pnas.0404603101.

Watson, P.J., Fairall, L., Santos, G.M., Schwabe, J.W.R., 2012. Structure of hdac3 bound to co-repressor and inositol tetraphosphate. Nature 481, 335–340. doi:10.1038/nature10728.

Zhang, L., Yuan, C., Wang, Y., Zhao, S., 2016. Histone deacetylases 3 (hdac3) is highly expressed in cervical cancer and inhibited by sirna. International Journal of Clinical and Experimental Pathology 9, 3600–3605.

Zhang, Y., Wang, H., Li, F., Xu, X., Chen, B., Zhang, T., 2020. Inhibitory effects of dulcitol on rat c6 glioma by regulating autophagy pathway. Natural Product Research 34, 1437–1441. doi:10.1080/14786419.2018.1512994.

Zhou, H., Wang, C., Ye, J., Chen, H., Tao, R., 2017. Design, virtual screening, molecular docking and molecular dynamics studies of novel urushiol derivatives as potential hdac2 selective inhibitors. Gene 637, 63–71. doi:10.1016/j.gene.2017.09.034.